Supporting Information

Tungsten Doping Reinforced Structure Stability of Single-Crystal Nickel-Rich $LiNi_{0.9}Co_{0.1}O_2$ Cathode

Zhen Xiao [a, †,], Anqi Chen [b, †], Ruojian Ma [b], Yongquan Zheng [b], Xiao-Dong Qi [c], Yu-Jie Guo [c,] *, Ruyi Fang [b], Yongping Gan [b], Xinping He [b], Xiaoxiao Lu [d], Jianping Xu [e], Hui Huang [b], Jun Zhang [b], Xinhui Xia [b], Wenkui Zhang [b], Sen Xin [c,] *, Yang Xia [b,] **

[a] *Key Laboratory of Rare Earth Optoelectronic Materials and Devices of Zhejiang Province, Institute of Optoelectronic Materials and Devices, China Jiliang University, Hangzhou, 310018, China*

[b] *College of Materials Science and Engineering, Zhejiang University of Technology, Hangzhou, 310014, China*

[c] *CAS Key Laboratory of Molecular Nanostructure and Nanotechnology, Institute of Chemistry, Chinese Academy of Sciences (CAS), Beijing 100190, P. R. China*

[d] *School of Materials Science and Engineering, Zhejiang Sci-Tech University, Hangzhou, 310018, China*

[e] *Evercos Battery Co. Ltd., Suichang 323300, China*

[†] *These authors contributed equally to this work.*

* *Corresponding authors: xiaozhen@cjlu.edu.cn (Z. Xiao); guoyujie@iccas.ac.cn (Y.-J. Guo); xinsen08@iccas.ac.cn (S. Xin); nanoshine@zjut.edu.cn (Y. Xia)*

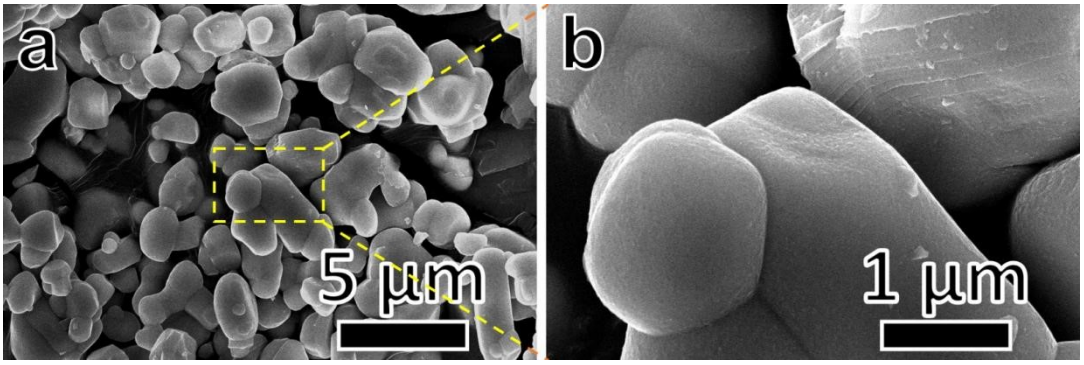

Figure S1. SEM images of pristine NC9010 after calcination at 750 ºC for 4 h.

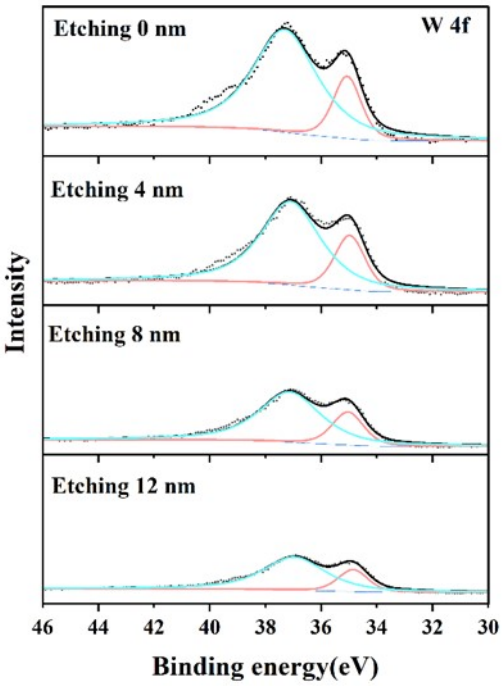

Figure S2. The XPS depth profile with etching 0, 4, 8, 12nm.

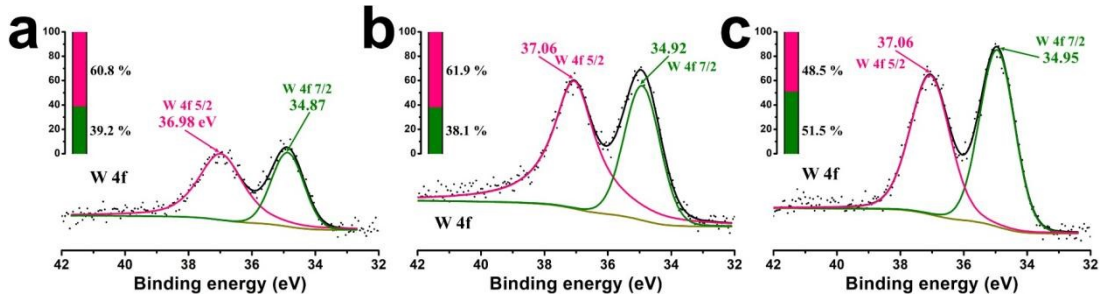

Figure S3. XPS results of W 4f regions in W-doping samples: (a) 0.3 mol% W doping, (b) 0.6 mol% W doping, and (c) 0.9 mol% W doping.

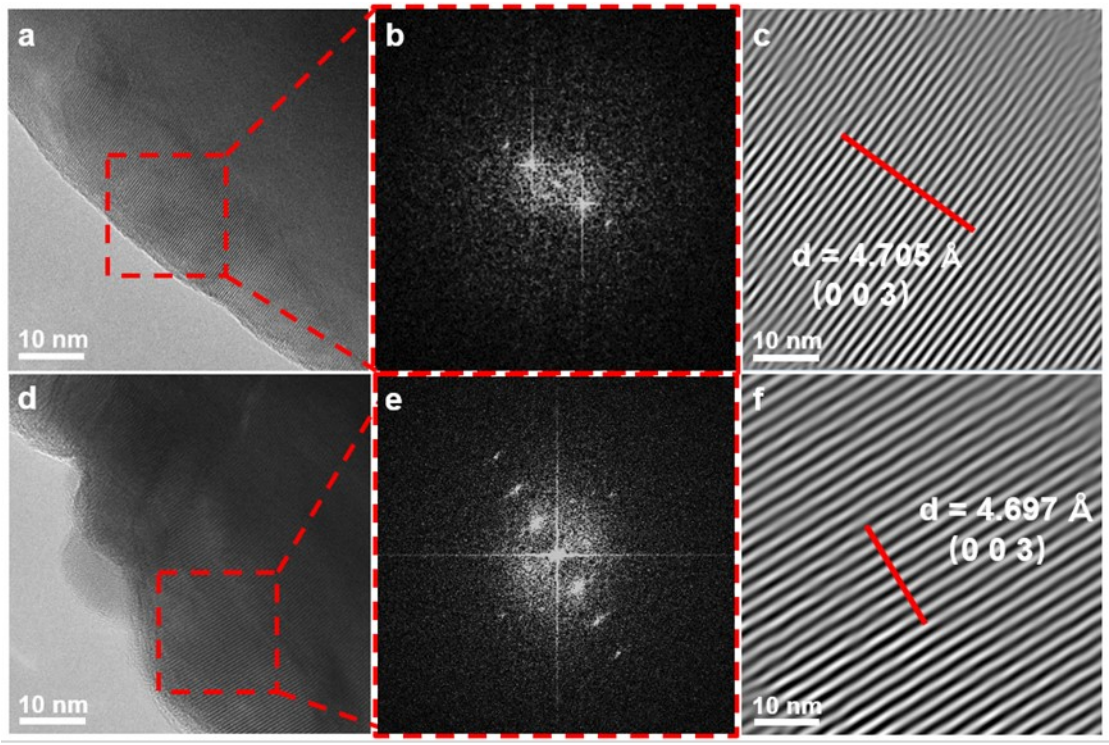

Figure S4. The HRTEM analysis for pristine (a-c) and 0.6 mol% W-doping sample (d-f).

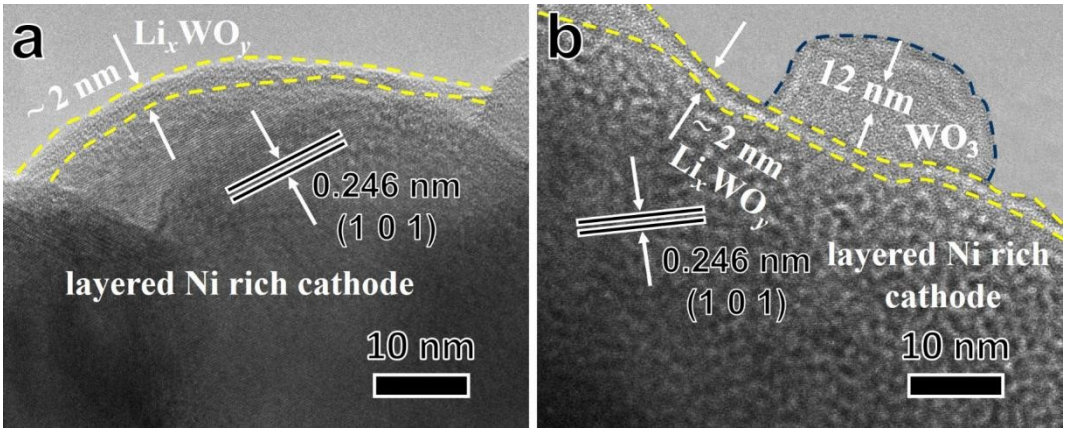

Figure S5. HRTEM images of (a) 0.6 mol% W doping and (b) 0.9 mol% W doping.

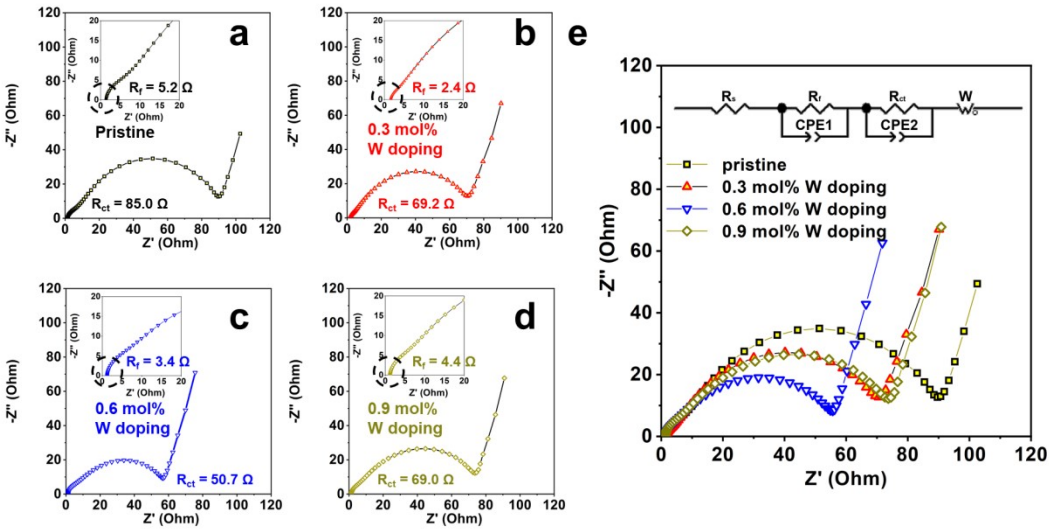

Figure S6. EIS curves and fitting analysis results of each sample before cycling (SOC = 0).

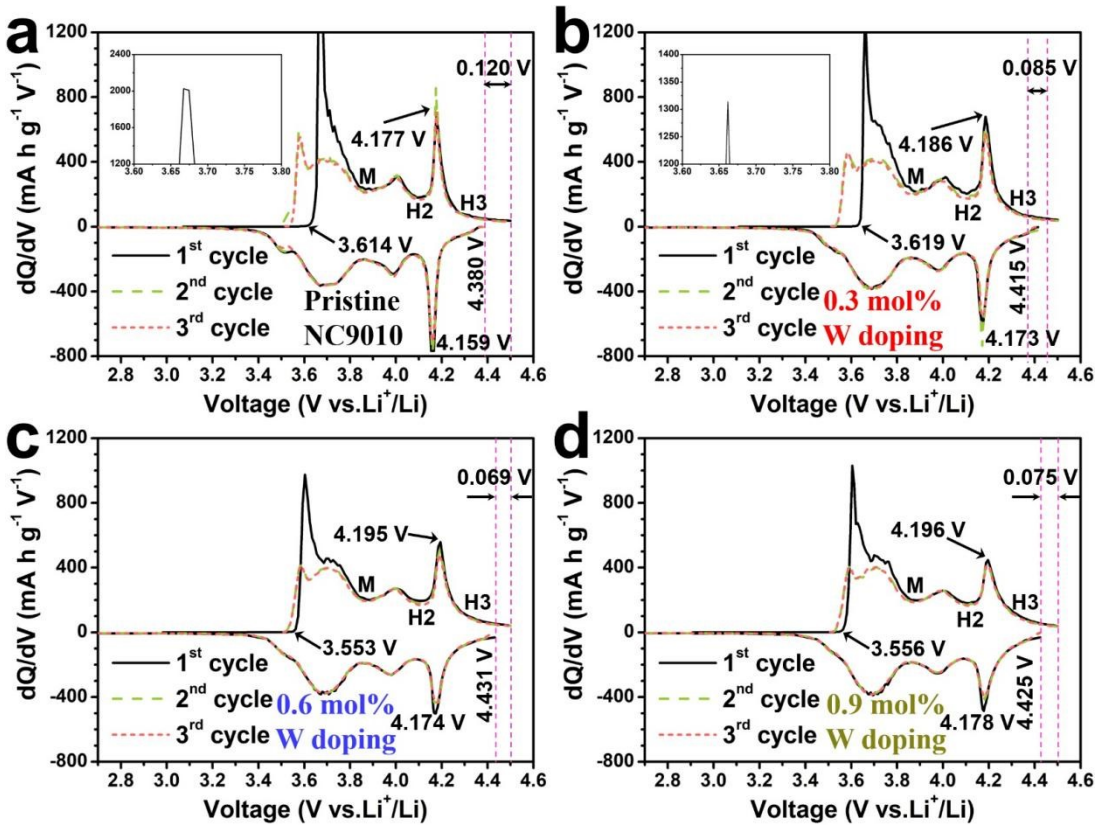

Figure S7. Differential capacity vs voltage curves for initial three cycles of (a) pristine, (b) 0.3 % W doping, (c) 0.6 % W doping, and (d) 0.9 % W doping.

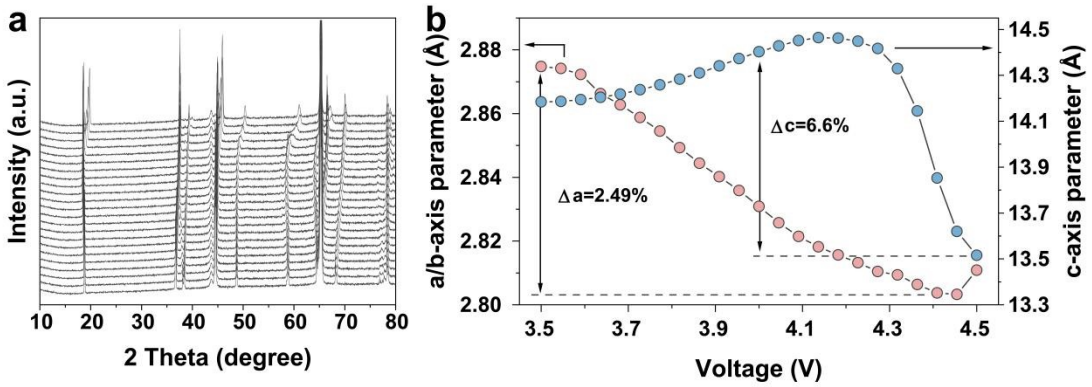

Figure S8. (a) *In-situ* XRD patterns during first charging process of pristine sample and (b) corresponding lattice parameter variations.

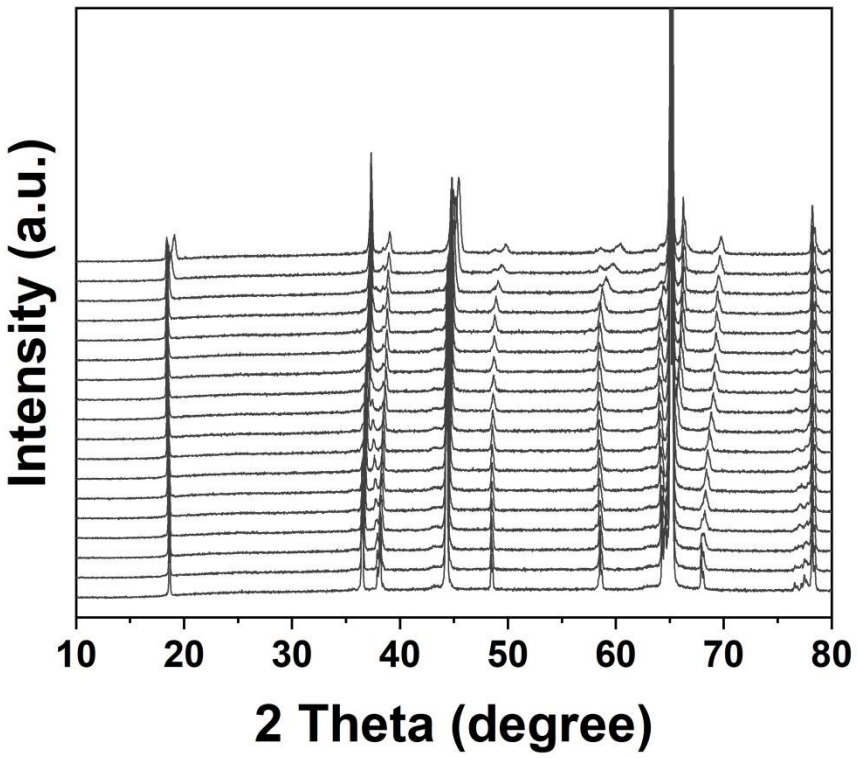

Figure S9. *In-situ* XRD patterns during first charging process of 0.6 mol% W-doping sample.

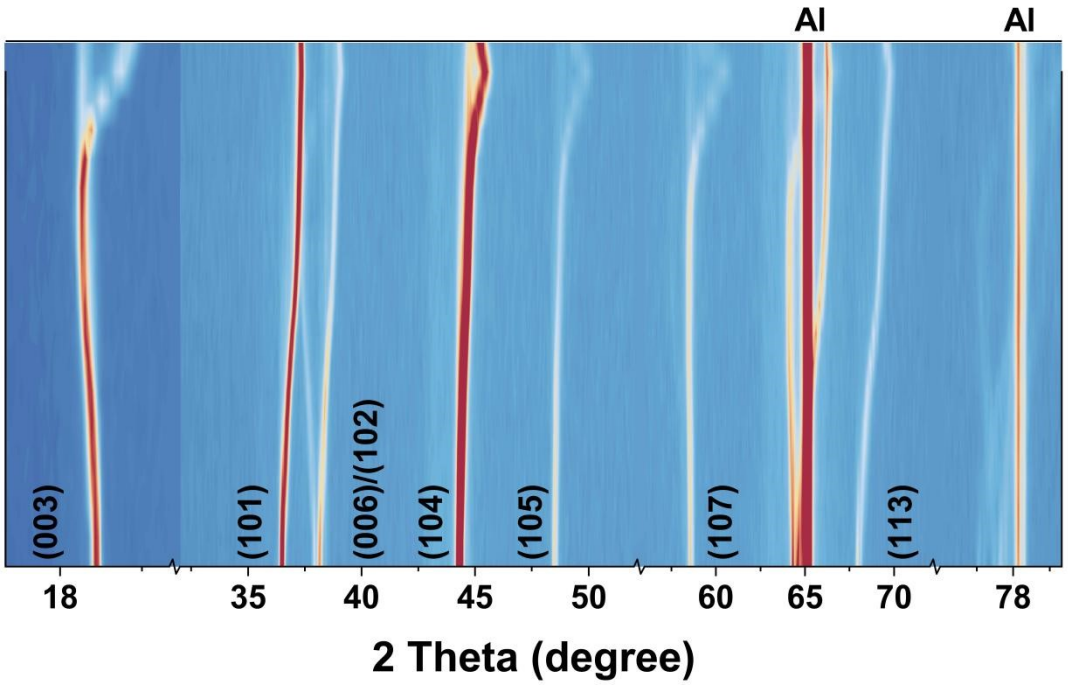

Figure S10. *In-situ* XRD patterns with contour plots of 0.6 mol% W-doping sample during first charging process.

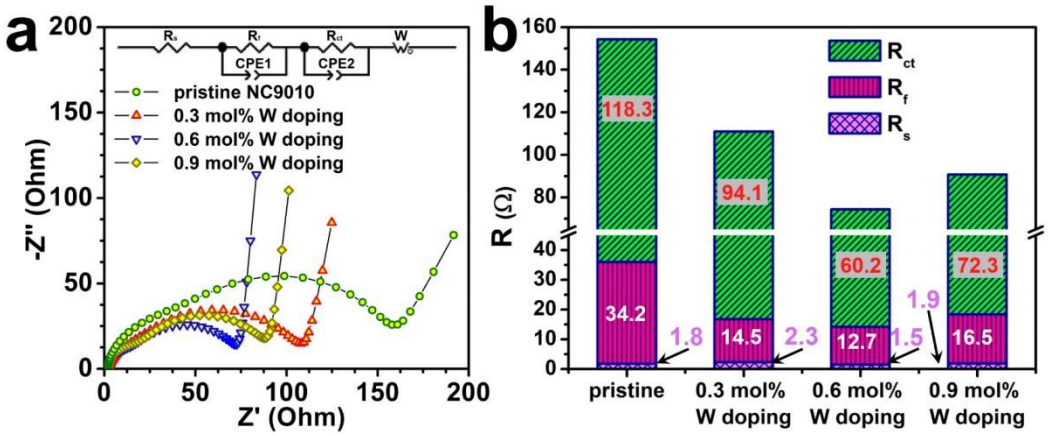

Figure S11. (a) EIS curves and (b) fitting analysis results of samples after 200 cycles (SOC = 0).

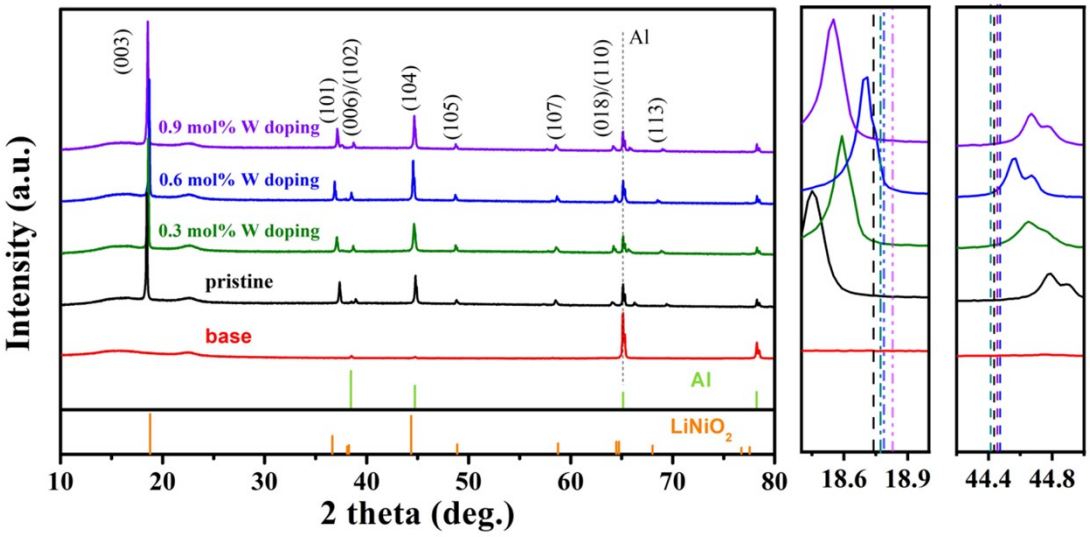

Figure S12. XRD patterns of cathodes after cycling at 0.5 C.

Table S1. The (003) and (104) peaks shift of various samples after cycles

Sample	(003)	(104)
Pristine	decrease 0.27 degree	increase 0.37 degree
0.3 mol% W doping	decrease 0.15 degree	increase 0.25 degree
0.6 mol% W doping	decrease 0.03 degree	increase 0.13 degree
0.9 mol% W doping	decrease 0.21 degree	increase 0.25 degree